Journal of Hazardous Materials 171 (2009) 484–490

Contents lists available at ScienceDirect

Journal of Hazardous Materials

journal homepage: www.elsevier.com/locate/jhazmat

Removal of Cr(VI) from polluted solutions by electrocoagulation: Modeling of experimental results using artificial neural network

S. Aber*, A.R. Amani-Ghadim[1], V. Mirzajani[1]

Environmental Protection Research Laboratory, Department of Applied Chemistry, Faculty of Chemistry, University of Tabriz, 29 Bahman Blvd., Tabriz, Iran

ARTICLE INFO

Article history:
Received 3 February 2009
Received in revised form 3 May 2009
Accepted 7 June 2009
Available online 16 June 2009

Keywords:
ANN
Chromium
Current density
Electrocoagulation
Electrolyte

ABSTRACT

In the present work, the removal of Cr(VI) from synthetic and real wastewater using electrocoagulation (EC) process was studied. The influence of anode material, initial Cr(VI) concentration, initial pH of solution, type of electrolyte, current density and time of electrolysis was investigated. During 30 min of electrocoagulation, maximum removal efficiencies achieved by Al and Fe anodes were 0.15 and 0.98, respectively. High removal efficiency was achieved over pH range of 5–8. NaCl, Na_2SO_4 and $NaNO_3$ were used as supporting electrolyte during the electrolysis. NaCl was more effective than Na_2SO_4 and $NaNO_3$ in removal of hexavalent chromium. Also in this work, a real electroplating wastewater containing 17.1 mg/l Cr(VI) was treated successfully using EC process. Artificial neural network (ANN) was utilized for modeling of experimental results. The model was developed using a 3-layer feed forward backpropagation network with 4, 10 and 1 neurons in first, second and third layers, respectively. A comparison between the model results and experimental data gave high correlation coefficient (R^2 = 0.976) shows that the model is able to predict the concentration of residual Cr(VI) in the solution.

1. Introduction

Water pollution by heavy metals, especially chromium; have sparked much concern to societies and regulation authorities around the world. Due to chromium wide usage by different industries such as metal plating, paints and pigments, leather tanning, textile dyeing, printing inks and wood preservation, huge quantity of wastewater containing chromium is discharged into the environment in trivalent (Cr(III)) and hexavalent (Cr(VI)) forms. The hexavalent chromium compounds are toxic and carcinogenic. In contrast, relative toxicity of Cr(III) is low and in its trace amounts, it is not a problem for the environment [1]. The most common method used for the removal of chromium from wastewater is the acidic reduction of Cr(VI) to Cr(III) (pH 2–3) followed by raising pH to precipitate the Cr(III) [2].

Electrochemical technology can be applied for the treatment of effluents released from a wide range of industries or processes. One of the electrochemical methods is electrochemically assisted coagulation, electrocoagulation (EC), that can compete with the conventional chemical coagulation process in the treatment of wastewaters [3]. The electrocoagulation has successfully been employed for treatment of different wastewaters such as wastewaters from laundries, restaurants, slaughterhouses, etc. [4–8]. Meanwhile, EC process has been used in the removal of phosphate [9], sulfide, sulfate and sulfite [10], fluoride [11] and boron [12].

EC includes in situ generation of coagulants through electrodissolution of either aluminum or iron electrodes. An iron anode results in release of Fe^{2+} or Fe^{3+}. Fe^{2+} can be oxidized to Fe^{3+} by more than one mechanism. The electrochemical reactions with metal M (Al or Fe) as anode may be summarized as follows [13,14]:

$$\text{At the anode}: \ M_{(s)} \rightarrow M^{n+}_{(aq)} + ne^- \quad (1)$$

$$\text{Atthecathode}: \ 2H_2O_{(l)} + 2e^- \rightarrow H_{2(g)} + 2OH^-_{(aq)} \quad (2)$$

In the bulk of solution, hydroxides and/or polyhydroxides of iron or aluminum are produced. Metallic pollutants precipitate as hydroxide flocs and other pollutants such as organic matters are adsorbed on these flocs. This mechanism helps to remove various kinds of contaminants from water [13–16]. According to the literature the benefits from using electrochemical techniques include [17]: (i) more effective and rapid pollutant removal than coagulation, (ii) pH control is not necessary, (iii) the amount of chemicals required is small and (iv) the operating costs are much lower than the most conventional technologies.

Modeling of electrocoagulation process has been little investigated. Hu and Kuan [18] specified the kinetics of the fluoride removal reaction by EC process using Langmuir equation. Emamjomeh and Sivakumar [11] developed empirical model using

* Corresponding author. Tel.: +98 411 3393153; fax: +98 411 3340191.
E-mail addresses: soheil_aber@yahoo.com (S. Aber), a.r_amani@yahoo.com (A.R. Amani-Ghadim), vahid.mirzajany@gmail.com (V. Mirzajani).
[1] Tel.: +98 411 3393153; fax: +98 411 3340191.

0304-3894/$ – see front matter © 2009 Elsevier B.V. All rights reserved.
doi:10.1016/j.jhazmat.2009.06.025

critical parameters for fluoride removal by monopolar ECF process. Den and Huang [15] employed a steady-state transport equation with second-order reaction kinetics to describe the rate of coagulation in electrocoagulation of silica nanoparticles in wafer polishing wastewater by a multichannel flow reactor. Canizares et al. [19,20] developed a mathematical model for the electrocoagulation process and tested it with experimental data obtained during the treatment of kaolin suspensions, dye polluted wastewaters and oil-in-water emulsions.

Wastewater treatment using EC process is, in general, complicated. This is caused by complex and synchronous reactions occurred during EC process, such as electrodissolution of anode, hydrolysis of metal ions, formation of the hydroxyl complexes, adsorption of pollutants on amorphous metal hydroxide precipitates, etc. [14]. Since the process depends on several factors, the modeling of these processes has many problems which cannot be easily solved by simple linear multivariate correlation.

The artificial neural network ability to recognize and reproduce cause and effect relationships through training, for multiple input/output systems, makes it efficient to represent even the most complex systems [21]. Because of their reliable, robust and salient characteristics in capturing the non-linear relationships existing between variables (multi-input/output) in complex systems, numerous applications of ANN have been successfully conducted to solve environmental engineering problems [22–26].

For every ANN, the first layer constitutes the input layer (independent variables) and the last one forms the output layer (dependent variables). Between them, one or more neurons in layers, called hidden layers, can be located. The hidden layers act as feature predictors and, in theory, there can be more than one hidden layer. Information in an ANN is distributed among multiple cells (nodes) and connections between the cells (weights) [27].

The universal approximation theory, suggests that for a network with more inputs than outputs, one hidden layer is enough [28]. In the feed-forward neural network the inputs are presented to the ANN at the input layer and then weighted by the connections between the input and hidden layer. Hidden layer perform two tasks: a summation of the weighted inputs followed by an insertion of this sum on a transfer function f_h, to produce a response. In turn, hidden nodes responses are weighted by the connections between the hidden and output layer and forwarded to the nodes of the output layer. Similarly to hidden nodes, output nodes perform a summation of incoming weighted signals and project the sum on their specific transfer function f_0. The output of each output node is the estimated responses, y_{pred}, that can be expressed as [27]:

$$y_{pred} = f_0 \left[\theta'' + \sum_{j=1}^{nh} w''_j f_h \left(\sum_{i=1}^{nd} w'_i x_i + \theta' \right) \right] \quad (3)$$

where nd and nh are the number of input variables and hidden nodes, respectively. Adjustable parameters are the weights $w\prime_i$, $w\prime\prime_j$ and biases θ', θ'' that act as offset terms by shifting the transfer functions horizontally. They are determined with an iterative procedure called training or learning. The adjustable parameters are first ascribed initial random values, then training starts and proceeds in two steps. First, a forward pass is performed through the ANN with a set of training samples with known experimental response, y_{exp}. At the end of the pass, the magnitude of the error between experimental and predicted responses is calculated and used to adjust all weights of the ANN, in a backpropagation step. A new forward pass is then performed with the training samples and the optimized parameters. The whole procedure is repeated until convergence is reached [27,28]. The most widely used transfer function for the hidden layer (f_h) is the sigmoid transfer function and is given by [29]:

$$f(x) = \frac{1}{1 + e^{-x}} \quad (4)$$

The linear transfer function is used as the output layer transfer function (f_0).

To the best of our knowledge, removal of Cr(VI) by EC was not modeled yet because EC process is, in general, complicated. This study discusses the use of a multilayer feed-forward neural network model to predict the removal of Cr(VI) from solution by EC process. For this purpose, we needed to have some experimental data as training, validation and test sets. The sets included current density, time of electrolysis, initial Cr(VI) concentration and sodium chloride concentration as input data and residual Cr(VI) concentration as output data. Therefore, some experiments were done to find the output parameter versus input parameters. Before obtaining the data to be used in modeling, the proper values of other important effective parameters such as electrode material, initial pH and type of electrolyte were found and kept constant in experimental and modeling procedures.

2. Materials and methods

2.1. Materials and instruments

The Cr(VI) solution was prepared by dissolving potassium dichromate (Merck, Germany) in distilled water. The conductivity of solutions (γ) was raised up and adjusted by adding one of NaCl, Na_2SO_4 or $NaNO_3$ salts as electrolyte (Fluka, Switzerland). The conductivity measurement was carried out using a Philips conductivity meter (PW 9509, England). The pH of the solutions was measured by pH meter (Metrohm 654, Switzerland) and adjusted by adding NaOH or HCl (Merck, Germany) solutions. Iron (ST 37-2) or aluminum (HE 18) plates were used as anode, and steel (grade 304) plates were used as cathode. Dimensions of electrodes were 40 mm × 50 mm × 1 mm. The electrodes were connected to a DC power supply (ADAK PS808, Iran) with galvanostatic operational option to control the current density.

2.2. General procedure

The experimental set-up is shown in Fig. 1. The distance between two electrodes in EC cell was 15 mm in all experiments. All the runs were performed at room temperature. In each run 500 ml of Cr(VI) solution (with specified concentration) or real wastewater was placed into the electrolytic cell. The operation started when the current density was adjusted to a desired value. During the process, the solution was agitated at 200 rpm and the sampling was carried out. The samples were filtered through 0.2 μm membrane filter (Schliecher & Schuell, Germany). The concentration of Cr(VI) in solution was analyzed spectrophotometrically using 1,5-diphenylcarbazide according to the standard method for the examination of water and wastewater [30]. The intensity of the color of Cr(VI)-diphenylcarbazide complex in the solution was measured at 540 nm using UV–Vis spectrophotometer (Perkin-Elmer 550 SE). The total amount of chromium and nickel in solution was measured by flame atomic absorption spectrophotometer (AAS) (Konik 210 VGP). The removal efficiency (X) was calculated using Eq. (5) where C_0 is the initial concentration of Cr(VI) and C is concentration of Cr(VI) at time t

$$X = \left(1 - \frac{C}{C_0}\right) \quad (5)$$

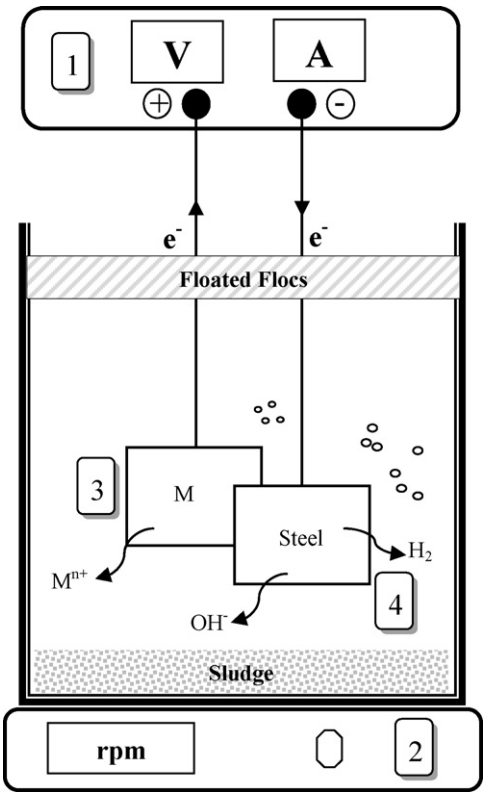

Fig. 1. Schematic diagram of the electrocoagulation reactor. (1) Digital DC power, (2) magnetic bar—stirrer, (3) anode, and (4) cathode.

2.3. Artificial neural network (ANN)

In this work, multilayer feed-forward ANN with one hidden layer was used. For all data sets, sigmoid transfer function in the hidden layer and a linear transfer function in the output node were used. The ANN was trained using the backpropagation algorithm. All calculations were carried out with Matlab mathematical software with the ANN toolbox. Current density (j), time of electrolysis (t_{EC}), initial concentration of Cr(VI) and the concentration of electrolyte were used as inputs of ANN model.

Total 212 experimental points were randomly split between training, validation and test sets. That is 128, 42, 42 points were used as training, validation and test sets, respectively. All samples were normalized in the 0.1–0.9 range. So, all of the data (x_i) (from training, validation and test sets) were converted to normalized values (x_{norm}) as follows [21,28]:

$$x_{norm} = 0.8\left(\frac{x_i - x_{\min}}{x_{\max} - x_{\min}}\right) + 0.1 \quad (6)$$

3. Results and discussion

3.1. Comparing performance of iron and aluminum as anode material

In any electrochemical process, electrode material has significant effect on the treatment efficiency. Therefore, appropriate selection of the electrode material is important. Iron and aluminum are the most common electrode materials used in EC processes. To investigate the effect of electrode materials on the removal efficiency, electrocoagulation process was carried out using iron and aluminum anodes. Fig. 2 shows the removal efficiency of Cr(VI) and total chromium versus time. It can bee seen that, the iron electrode is more efficient than aluminum electrode and during 30 min

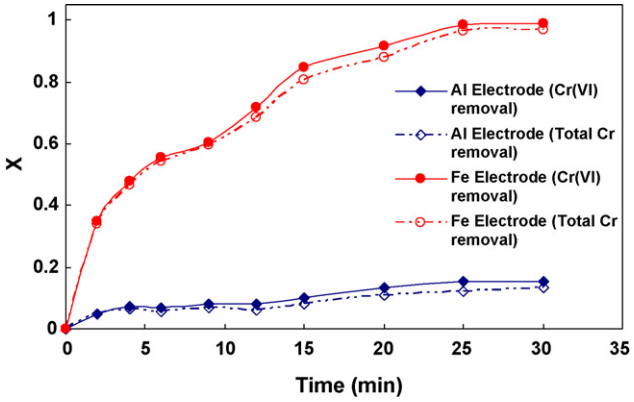

Fig. 2. Effect of electrode material on the removal efficiency of total Cr and Cr(VI). (j = 50 A/m^2, pH 5, [Cr(VI)]$_0$ = 50 mg/l, [NaCl]$_0$ = 10 g/l, γ = 16.27 mS/cm and stirring speed = 200 rpm).

of electrocoagulation, maximum removal efficiency achieved by Al electrode is only 0.15. The less removal efficiency of Al electrode than Fe electrode can be explained by main reactions occurs in EC process. Anodic process includes the dissolution (oxidation) of iron or aluminum [13]:

$$Fe_{(s)} \rightarrow Fe_{(aq)}^{2+} + 2e^- \quad (7)$$

$$Fe_{(s)} \rightarrow Fe_{(aq)}^{3+} + 3e^- \quad (8)$$

$$Al_{(s)} \rightarrow Al_{(aq)}^{3+} + 3e^- \quad (9)$$

The corresponding cathodic half-reactions are water reduction (Eq. (2)) and direct electrochemical metal reduction [2]:

$$Cr_2O_7^{2-} + 6e^- + 14H^+ \rightarrow 2Cr^{3+} + 7H_2O \quad (10)$$

Moreover, there are several reactions occurs in the bulk of the solution. Fe^{2+} which is produced on the anode reduces Cr(VI) to Cr(III) [2,31]:

$$Cr_2O_7^{2-} + 6Fe^{2+} + 14H^+ \rightarrow 2Cr^{3+} + 6Fe^{3+} + 7H_2O \quad (11)$$

If oxygen is formed on the anode, it is able to oxidize dissolved Fe^{2+} to Fe^{3+} [13,14]:

$$4Fe_{(aq)}^{2+} + 2H_2O_{(l)} + O_{2(g)} \rightarrow 4Fe_{(aq)}^{3+} + 4OH_{(aq)}^- \quad (12)$$

Subsequently, the hydroxide ions formed on the cathode increase the pH of the solution and may cause precipitation of Cr(III) and the cations released from anode in the form of their corresponding hydroxides.

Based on Eqs. (10) and (11) Cr(VI) ions can be reduced by two paths: (i) electrochemical reduction at the cathode surface (Eq. (10)). (ii) electrochemical reduction by Fe^{2+} ions produced on the anode (Eq. (11)). It is known that the Al^{3+} ions, released from Al anode, could not reduce Cr(VI) to Cr(III). So, it can be concluded that the electrochemical reduction of chromate ions by Fe^{2+}, released from iron anode, is the important step in the removal of chromate by EC process and the majority of Cr(VI) is reduced by Fe^{2+} ions (type of the cathode was the same in all experiments). Accordingly, all later experiments carried out using iron anode. Fig. 2 shows that total chromium removal was almost the same as the Cr(VI) removal. So, it can be resulted that the Cr(III) is almost completely removed from solution, and efficiently (co-)precipitated with the iron or aluminum hydroxides.

3.2. Effect of initial pH on the removal efficiency of Cr(VI) and total chromium

The dependence of removal efficiency on initial pH values was studied over pH range of 1–11. It can be seen from Fig. 3 that the ini-

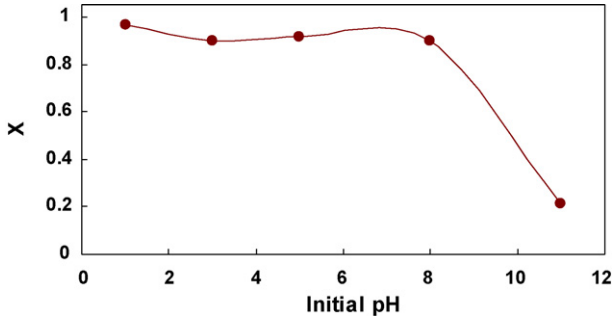

Fig. 3. Effect of initial pH on the removal efficiency of Cr(VI). (Anode material: iron, $j = 50\ A/m^2$, $t_{EC} = 30$ min, $[Cr(VI)]_0 = 50$ mg/l, $[NaCl]_0 = 10$ g/l, $\gamma = 16.27$ mS/cm and stirring speed = 200 rpm.)

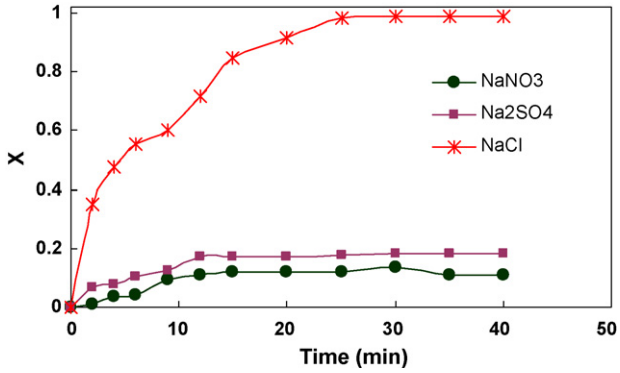

Fig. 4. Effect of electrolyte type on the removal efficiency of Cr(VI) ($j = 50\ A/m^2$, pH 5, $[Cr(VI)]_0 = 50$ mg/l, [Electrolyte] = 10 g/l and stirring speed = 200 rpm).

tial pH has significant effect on the removal efficiency of Cr(VI). At the pH > 9 removal efficiency decreased more than 80%. The plausible reason for less Cr(VI) removal in more basic conditions could be that the reduction of Cr(VI) to Cr(III) requires H^+ ions (Eq. (11)). Consequently, at alkaline pH values, reaction between Fe^{2+} and Cr(VI) occurs very slowly.

According to Fig. 3, the maximum removal efficiency of Cr(VI) (X = 0.97) was achieved at high acidic mediums. For initial high acidic conditions (pH 1) and initial Cr(VI) concentration of 50 mg/l after 30 min, the results (Table 1) indicate that residual total chromium concentration and final pH are 49 mg/l and 2.1, respectively. In the presence of high H+ concentration, Cr(VI) ions is only reduced to Cr(III) ions and could not be precipitated. So, in more acidic conditions, the removal efficiency of total chromium is negligible while the efficiency for Cr(VI) removal is high. From Table 1 and Fig. 3, it can be concluded that over pH range of 5–8, the majority of Cr(VI) is precipitated in the form of Cr(OH)3 and proper removal of both Cr(VI) and total chromium can be achieved in this range of pH. So, it is the optimum pH range for removal of Cr(VI) and total chromium using EC process. Since the initial pH value of the Cr(VI) solutions was around 5, there was no need to change the pH of the solutions and all later experiments were done at this initial pH value.

3.3. Effect of electrolyte type on the removal efficiency of Cr(VI)

In order to reduce the IR-drop or solution resistance potential (η_{IR}), conductivity of the solution should be sufficient. Most electrocoagulation studies have used chloride as anion to enhance the conductivity of the solution and some of them have utilized nitrate and sulphate as the electrolyte [2,13,32]. To study the effect of electrolyte type on the removal efficiency of Cr(VI), its removal by EC using iron electrodes in the presence of different supporting electrolytes including NaCl, Na_2SO_4 and $NaNO_3$ was studied. Current density of 50 A/m^2 and electrolyte concentration of 10 g/l were uniformly applied to the experiments. It can be seen from Fig. 4 that in the presence of NaCl the removal efficiency of Cr(VI) was 0.99 at the electrolysis time of 30 min. This is compared with the removal efficiencies of 0.18 and 0.14 for the same experiments performed in the presence of Na_2SO_4 and $NaNO_3$ as electrolyte, respectively. The difference could be attributed to the passivation of electrodes. It is known that immersion of metallic iron in Cr(VI) solution at open circuit leads to impenetrable passive chromite film that affect the anodic dissolution of iron. However in the presence of chloride ion, the passivation is curtailed since the adsorbed chloride ion promotes the dissolution of iron [33]. The data presented in Table 2 confirm that chloride ions increase the oxidation of iron electrode. Current efficiency with respect to Fe dissolution relates to the ratio of the actual amounts of Fe dissolution (Δm_{theo}) to that expected theoretically from Faraday's law (Eq. (13)). Faraday's formula can be expressed as

$$\Delta m_{theo} = \frac{MIt_{EC}}{nF} \quad (13)$$

where I is the current (A), t_{EC} is the time of electrolysis (s), m is the amount of iron dissolved (g), M is the atomic weight of the iron (g/mol), n is the number of electron moles (in Eq. (7)) and F is the Faraday's constant ($F = 96{,}487$ C/mol).

The current efficiency (φ) of EC process was calculated (Eq. (14)) based on the comparison of experimental weight loss of iron electrodes (Δm_{exp}) during EC process with theoretical amount of iron dissolution (Δm_{theo}) according to the Faraday's law (Eq. (13))

$$\varphi = \frac{\Delta m_{exp}}{\Delta m_{theo}} \quad (14)$$

Comparison of current efficiencies revealed that sulfate and nitrate ions have less influence on corrosion of iron than chloride (Table 2). In the presence of these ions dissolution of iron electrode was very low and Cr(VI) ions only are reduced at the cathode. Cl^- ions decrease the passivity of the electrodes by removing the passivating oxide layer formed on electrode surface due to its catalytic action [33]. Investigation on the effect of sodium chloride concentration on the removal efficiency showed that during 30 min electrocoagulation, an increase in the electrolyte concentration from 2.5 to 10 g/l yields an increase in the removal efficiency from 0.89 to 0.99 at current density equal to 50 A/m^2. Accordingly, electrolyte concentration has a little impact on removal efficiency in comparison with other operational parameters such as current density.

Table 1
Effect of initial pH on the final pH and residual total Cr concentration ($j = 50\ A/m^2$, $t_{EC} = 30$ min, $[Cr(VI)]_0 = 50$ mg/l, $[NaCl]_0 = 10$ g/l, $\gamma = 16.27$ mS/cm and stirring speed = 200 rpm).

Initial pH	Final pH	Total Cr concentration (mg/l)
1	2.1	49.0
3	8.2	20.1
5	9.1	1.5
8	9.6	7.1
11	11.4	40.2

Table 2
Effect of electrolyte type on the residual total Cr (mg/l) and current efficiency in EC process after 40 min ($j = 50\ A/m^2$, $[Cr(VI)]_0 = 50$ mg/l and stirring speed = 200 rpm).

Electrolyte	φ	γ (mS/cm)	Cell voltage (V)	Initial pH	Final pH	Total Cr (mg/l)
$NaNO_3$	0.07	11.09	4.8–5	4.8	5.9	45
Na_2SO_4	0.071	12.17	4.3–4.5	4.5	5.5	49
NaCl	0.99	16.27	2.2–2.3	5	9.1	0.90

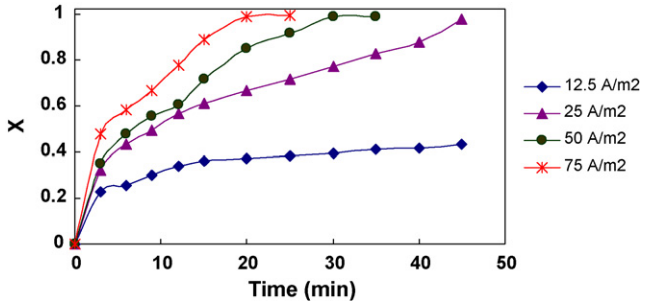

Fig. 5. Variation of Cr(VI) removal efficiency with time at different current densities; $[Cr(VI)]_0 = 50$ mg/l, pH 5, $[NaCl]_0 = 10$ g/l, $\gamma = 16.27$ mS/cm, and stirring speed = 200 rpm.

3.4. Effects of current density and time of electrolysis on the removal efficiency of Cr(VI)

According to Faraday's law (Eq. (13)), it is clear that amount of Fe^{2+} (Δm_{theo}) released from anode depends on the electrolysis time and current. So in the electrocoagulation process, current and electrolysis time are the most important parameters affecting the removal efficiency and controlling the reaction rate. To investigate the effects of current density and time of electrolysis on the Cr(VI) removal, a series of experiments were carried out by solutions containing a constant Cr(VI) concentration (50 mg/l) with current density varied from 12.5 to 75 A/m^2. Fig. 5 shows the Cr(VI) removal efficiency versus the electrolysis time for different current densities. As the results indicate, the removal efficiency increased with an increase in current density and time of electrolysis. During 30 min of electrocoagulation, the removal efficiency increased to about 0.99 at 75 A/m^2 from about 0.39 at 12.5 A/m^2. Also, an increase in the time of electrolysis from 9 to 30 min yields an increase in the removal efficiency from about 0.55 to about 0.99 at current density equal to 50 A/m^2. In other words, increase in current density and/or electrolysis time cause to improvement in the removal efficiency. At lower current densities, the less iron is released from the anode and hence the removal efficiency of Cr(VI) is low. Comparison of different current densities shows that 50 A/m^2 is optimum one and so, this value was applied to later experiments.

3.5. The effect of initial Cr(VI) concentration on its removal efficiency

The solutions with different initial Cr(VI) concentrations in the range of 20–80 mg/l were treated by EC using iron electrodes in the current density of 50 A/m^2. As the results indicate (Fig. 6), the removal efficiency of Cr(VI) decreased with an increase in its initial concentration. The reason is deducible from Faraday's law (Eq. (13)). According to Faraday's law, when current density and time are the same, the constant amount of Fe^{2+} is released to the solution. As a result, the Fe^{2+} ions produced at high initial Cr(VI) concentrations are insufficient to reduce all of the Cr(VI) ions.

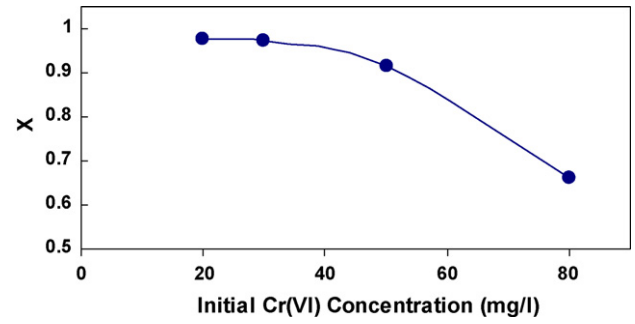

Fig. 6. Effect of initial Cr(VI) concentration on its removal efficiency ($j = 50$ A/m^2, pH 5, $[NaCl]_0 = 10$ g/l, $\gamma = 16.27$ mS/cm and stirring speed = 200 rpm).

Table 3
Characteristics of the electroplating wastewater before and after treatment by EC (anode material: iron, $j = 50$ A/m^2, $t_{EC} = 30$ min, stirring speed = 200 rpm).

Parameter	Value	
	Before treatment	After treatment
Total Cr (mg/l)	17.1	0.52
Total Ni (mg/l)	4.3	0.1
COD (mg/l)	280	38
Conductivity (mS/cm)	0.88	0.672
TDS (mg/l)	405	334
pH	6.9	10.1

3.6. Treatment of real electroplating wastewater containing Cr(VI)

In order to investigate the efficiency of EC process in the treatment of real wastewater containing Cr(VI), wastewater sample was obtained from an electroplating factory. The characteristics of the real wastewater are presented in Table 3. The treatment of real wastewater was performed at the current density equal to 50 A/m^2. After 30 min electrolysis, removal efficiency of total chromium, nickel and COD was 0.97, 0.98 and 0.86, respectively. The results presented in Table 3 show that electrocoagulation process can be used for efficient removal of total chromium and other pollutants from real wastewaters.

3.7. ANN modelling

The input variables to feed-forward neural network were the current density (over range of 12.5–75 A/m^2), time of electrolysis (over range of 0–45 min), initial concentration of Cr(VI) (over range of 20–80 mg/l) and concentration of sodium chloride (over range of 2.5–10 g/l). The residual Cr(VI) concentration was the experimental response or output variable. It was between zero and 80 mg/l.

The topology of an artificial neural network (ANN) is determined by the number of layers, the number of nodes in each layer and the nature of the transfer functions. Correct identification of the set of independent input variables and the output variables is the first task in the building ANN model. Optimization of ANN topology is the next important step in the development of a model. The number of neurons (N) in the hidden layer is determined according to the minimum prediction error of the neural network. Hence, it may be considered as a parameter for the neural network design [21]. In order to determine the optimum number of hidden nodes, different topologies were examined, in which the number of nodes was varied from 2 to 20. Each topology was repeated three times.

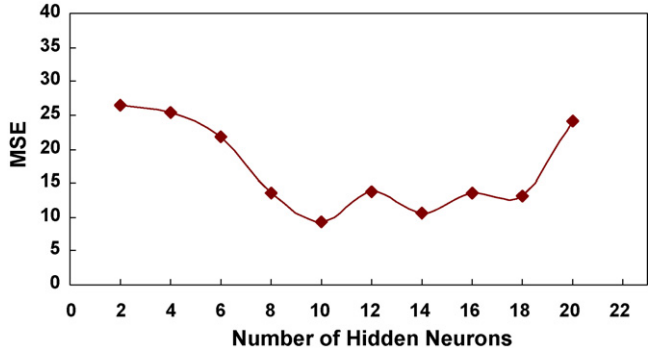

Fig. 7. Variation of MSE versus number of neurons in hidden layer.

Table 4
Matrix of weights between input and hidden layers in optimized ANN.

Neuron	N_1	N_2	N_3	N_4	N_5	N_6	N_7	N_8	N_9	N_{10}
Weights of connection from j	−0.51796	1.4006	−1.3623	1.7552	−2.8791	1.5934	−0.45388	−3.2752	−1.7416	−3.0451
Weights of connection from t_{EC}	4.4805	2.2913	−0.97459	2.7322	1.6293	−2.922	2.3521	0.58327	−2.4354	−3.3986
Weights of connection from $[Cr(VI)]_0$	−0.91785	−3.8203	2.2472	−3.3621	4.8438	−1.3042	2.9719	2.2822	−2.416	−3.7156
Weights of connection from $[NaCl]_0$	−0.92306	−3.6248	−2.6957	−2.4866	2.2928	5.7728	−6.4457	0.89139	−4.9693	−2.8968
Bias in hidden layer	2.0382	−1.4316	2.6232	−1.3461	−2.9701	0.67584	1.3139	−2.3629	4.0963	2.359

Table 5
Matrix of weights between hidden and output layers.

Neuron	N_1	N_2	N_3	N_4	N_5	N_6	N_7	N_8	N_9	N_{10}
Weights	−0.93118	0.21766	0.2483	0.55837	−0.04605	0.38373	−0.18993	0.21699	0.26544	−0.78226
Bias in output layer	1.0036									

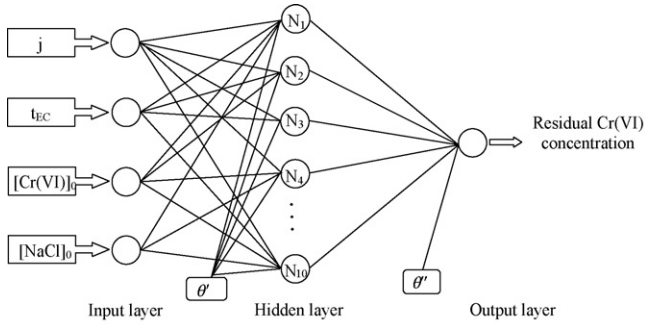

Fig. 8. ANN optimized structure.

Fig. 7 illustrates the network error versus the number of neurons in the hidden layer. It could be seen that the network mean square error (MSE) is minimum with inclusion of ten nodes in the hidden layer. So, based on the approximation of MSE function, a number of hidden neurons equal to ten was adopted and a three-layer feed-forward backpropagation neural network was used for the modeling of the process (Fig. 8). The MSE was used as the error function. It measures the performance of the network according to the following equation [21,25]:

$$MSE = \frac{1}{N}\sum_{i=1}^{i=N}(y_{i,pred} - y_{i,\exp})^2 \quad (15)$$

where N is the number of data points, $y_{i,pred}$ is the network prediction, $y_{i,exp}$ is the experimental response and i is an index of data.

The weights provided by ANN listed in Tables 4 and 5. The network was evaluated by comparing its predicted output values with the experimental ones using an independent set of data (test set). Fig. 9 demonstrates the plot of the experimental results (test set) versus the predicted ones. It shows that the points are well distributed around $X = Y$ line in a narrow area. A correlation coefficient of $R^2 = 0.976$ for the line plotted using experimental and calculated data, indicates the reliability of the model.

The weight matrix can be employed to evaluate the relative importance of the input variables on the output variable. For this purpose, Eq. (16) can be used based on the partitioning of connection weights [34,35]:

$$I_g = \frac{\sum_{m=1}^{m=N_h}\left(\left(\frac{|W_{gm}^{ih}|}{\sum_{k=1}^{N_i}|W_{km}^{ih}|}\right)\times|W_{mn}^{ho}|\right)}{\sum_{k=1}^{k=N_i}\left\{\sum_{m=1}^{m=N_h}\left(\left(\frac{|W_{gm}^{ih}|}{\sum_{k=1}^{N_i}|W_{km}^{ih}|}\right)\times|W_{mn}^{ho}|\right)\right\}} \quad (16)$$

where I_g is the relative importance of the gth input variable on the output variable, N_i and N_h are the numbers of input and hidden neurons, respectively, W is connection weight, the superscripts 'i', 'h' and 'o' refer to input, hidden and output layers, respectively, and subscripts 'k', 'm' and 'n' refer to input, hidden and output neuron numbers, respectively.

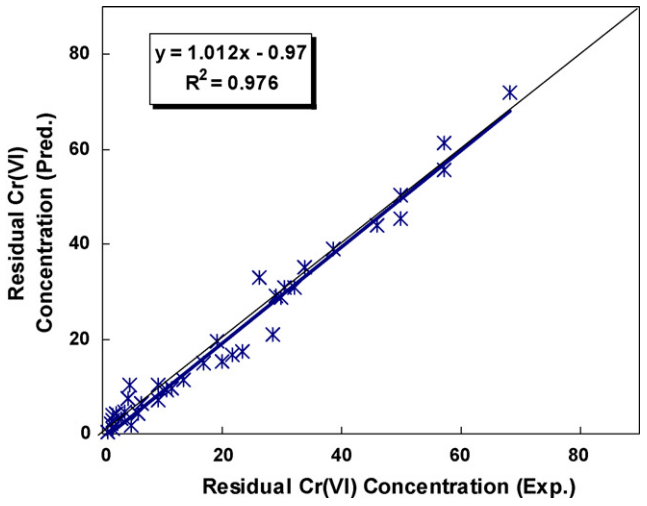

Fig. 9. Predicted residual Cr(VI) concentrations (using ANN) versus experimental ones.

For the current density, time of electrolysis, initial concentration of Cr(VI) and concentration of sodium chloride the relative importance as calculated by Eq. (16) were 16.51, 32.36, 23.83 and 27.03, respectively. So, all of the input variables have strong effect on the removal of Cr(VI) and none of the variables studied could be disregarded in the present modeling.

4. Conclusion

The electrocoagulation process was utilized for removal of Cr(VI) from synthetic and real wastewater which results in following conclusions:

(i) The EC process using iron anode can remove up to 97% of total chromium in the polluted solutions.
(ii) Iron anode has more removal efficiency for chromium removal than aluminum one which is because of electrochemical reduction of chromate ion by Fe^{2+}, produced from iron anode. Cr(VI) is significantly reduced to trivalent chromium in the presence of NaCl as supporting electrolyte while the reduction is negligible in the persence of $NaNO_3$ and Na_2SO_4 electrolytes.
(iii) At pH range of 5–8, the majority of Cr(VI) is precipitated in the form of $Cr(OH)_3$ and it is the optimum pH range for the removal of Cr(VI) and total chromium.

(iv) The performance of EC process in removal of Cr(VI) can be successfully predicted by applying a three-layer neural network (using a backpropagation algorithm) with four, ten and one neurons in input, hidden and output layers, respectively.

Acknowledgments

The authors are grateful to the University of Tabriz for financial and other supports. They are also grateful to M. Zarei and M.S. Seyed Dorraji for providing assistance during the stages of this study.

References

[1] Z. Yue, S.E. Bender, J. Wang, Economy, removal of chromium Cr(VI) by low-cost chemically activated carbon materials from water, J. Hazard. Mater. 166 (2009) 74–78.
[2] I. Heidmann, W. Calmano, Removal of Cr(VI) from model wastewaters by electrocoagulation with Fe electrodes, Sep. Purif. Technol. 61 (2007) 15–21.
[3] A.E. Yilmaz, R. Boncukcuoglu, M.M. Kocakerim, A quantitative comparison between electrocoagulation and chemical coagulation for boron removal from boron-containing solution, J. Hazard. Mater. 149 (2007) 475–481.
[4] N. Adhoum, L. Monser, N. Bellakhal, J. Belgaied, Treatment of electroplating wastewater containing Cu^{2+}, Zn^{2+} and Cr (VI) by electrocoagulation, J. Hazard. Mater. 112 (2004) 207–213.
[5] J. Ge, J. Qu, P. Lei, H. Liu, New bipolar electrocoagulation–electroflotation process for the treatment of laundry wastewater, Sep. Purif. Technol. 36 (2004) 33–39.
[6] E. Vorobiev, O. Larue, C. Vu, B. Durand, Electrocoagulation and coagulation by iron of latex particles in aqueous suspensions, Sep. Purif. Technol. 31 (2003) 177–192.
[7] X. Chen, G. Chen, P.L. Yue, Separation of pollutants from restaurant wastewater by electrocoagulation, Sep. Purif. Technol. 19 (2000) 65–76.
[8] M. Kobya, E. Senturk, M. Bayramoglu, Treatment of poultry slaughterhouse wastewaters by electrocoagulation, J. Hazard. Mater. 133 (2006) 172–176.
[9] N. Bektas, H. Akbulut, H. Inan, A. Dimoglo, Removal of phosphate from aqueous solutions by electro-coagulation, J. Hazard. Mater. 106 (2004) 101–105.
[10] M. Murugananthan, G.B. Raju, S. Prabhakar, Removal of sulfide, sulfate and sulfite ions by electro coagulation, J. Hazard. Mater. 109 (2004) 37–44.
[11] M.M. Emamjomeh, M. Sivakumar, An empirical model for defluoridation by batch monopolar electrocoagulation/flotation (ECF) process, J. Hazard. Mater. 131 (2005) 118–125.
[12] A.E. Yilmaz, R. Boncukcuoglu, M.M. Kocakerim, B. Keskinler, The investigation of parameters affecting boron removal by electrocoagulation method, J. Hazard. Mater. B 125 (2005) 160–165.
[13] N. Daneshvar, A.R. Khataee, A.R. Amani Ghadim, M.H. Rasoulifard, Decolorization of C.I. acid yellow 23 solution by electrocoagulation process: investigation of operational parameters and evaluation of specific electrical energy consumption (SEEC), J. Hazard. Mater. 148 (2007) 566–572.
[14] M.Y.A. Mollah, P. Morkovsky, J.A. Gomes, G. Kesmez, M.J. Parga, D.L. Cocke, Fundamentals, present and future perspectives of electrocoagulation, J. Hazard. Mater. B 114 (2004) 199–210.
[15] W. Den, C. Huang, Electrocoagulation of silica nanoparticles in wafer polishing wastewater by a multichannel flow reactor: a kinetic study, J. Environ. Eng. 132 (2006) 1651–1658.
[16] H.K. Hansen, P. Nunez, D. Raboy, I. Schippacasse, R. Grandon, Electrocoagulation in wastewater containing arsenic: comparing different process designs, Electrochim. Acta 52 (2007) 3464–3470.
[17] C.A. Martinez-Huitle, E. Brillas, Decontamination of wastewaters containing synthetic organic dyes by electrochemical methods: a general review, Appl. Catal. B: Environ. 87 (2009) 105–145.
[18] C.L.S. Hu, W. Kuan, Simulation the kinetics of fluoride removal by electrocoagulation (EC) process using aluminum electrodes, J. Hazard. Mater. 145 (2007) 180–185.
[19] P. Canizares, F. Martinez, M.A. Rodrigo, C. Jimenez, C. Saez, J. Lobato, Modeling of wastewater electrocoagulation processes. Part I. General description and application to kaolin-polluted wastewaters, Sep. Purif. Technol. 60 (2008) 155–161.
[20] P. Canizares, F. Martinez, M.A. Rodrigo, C. Jimenez, C. Saez, J. Lobato, Modeling of wastewater electrocoagulation processes. Part II. Application to dye-polluted wastewaters and oil-in-water emulsions, Sep. Purif. Technol. 60 (2008) 147–154.
[21] A. Aleboyeh, M.B. Kasiri, M.E. Olya, H. Aleboyeh, Prediction of azo dye decolorization by UV/H_2O_2 using artificial neural networks, Dyes Pigm. 77 (2008) 288–294.
[22] S. Gob, E. Oliveros, S.H. Bossmann, A.M. Braun, R. Guardani, C.A.O. Nascimento, Modeling the kinetics of a photochemical water treatment process by means of artificial neural networks, Chem. Eng. Process. 38 (1999) 373–382.
[23] S. Lek, J.F. Guegan, Artificial neural networks as a tool in ecological modeling: an introduction, Ecol. Model. 120 (1999) 65–73.
[24] S. Cinar, T.T. Onay, A. Erdincler, Co-disposal alternatives of various municipal waste water treatment-plant sludge's with refuse, Adv. Environ. Res. 8 (2004) 477–482.
[25] D. Salari, N. Daneshvar, F. Aghazadeh, A.R. Khataee, Application of artificial neural networks for modeling of the treatment of wastewater contaminated with methyl tert-butyl ether (MTBE) by UV/H_2O_2 process, J. Hazard. Mater. B 125 (2005) 205–210.
[26] K. Yetilmezsoy, S. Demirel, Artificial neural network (ANN) approach for modeling of Pb(II) adsorption from aqueous solution by *Antep pistachio* (*Pistacia vera* L.) shells, J. Hazard. Mater. 153 (2008) 1288–1300.
[27] F. Despagne, D. Massart, Neural networks in multivariate calibration, Analyst 123 (1998) 157R–178R.
[28] F.A.N. Fernandes, L.M.F. Lona, Neural networks applications in polymerization processes, Braz. J. Chem. Eng. 22 (2005) 401–418.
[29] M.M. Hamed, M.G. Khalafallah, E.A. Hassanien, Prediction of wastewater treatment plant performance using artificial neural networks, Environ. Model. Softw. 19 (2004) 919–928.
[30] L.S. Clesceri, A.E. Greenberg, R.R. Trusell, Standard Methods for the Examination of Water and Wastewater, 17th ed., American Public Health Association, Washington, DC, 1989.
[31] T. Olmez, The optimization of Cr(VI) reduction and removal by electrocoagulation using response surface methodology, J. Hazard. Mater. 162 (2009) 1371–1378.
[32] I. Heidmann, W. Calmano, Removal of Zn(II), Cu(II), Ni(II), Ag(I) and Cr(VI) present in aqueous solutions by aluminium electrocoagulation, J. Hazard. Mater. 152 (2008) 934–941.
[33] P. Lakshmipathiraj, R.G. Bhaskar, M. Basariya, S. Parvathy, S. Prabhakar, Removal of Cr (VI) by electrochemical reduction, Sep. Purif. Technol. 60 (2008) 96–102.
[34] G.D. Garson, Interpreting neural-network connection weights, AI Expert 6 (1991) 47–51.
[35] D. Salari, A. Niaei, A.R. Khataee, M. Zarei, Electrochemical treatment of dye solution containing C.I. Basic Yellow 2 by the peroxi-coagulation method and modeling of experimental results by artificial neural networks, J. Electroanal. Chem. 629 (2009) 117–125.